Maximizing Energy Production from Hydropower Dams using Short-Term Weather Forecasts

Shahryar Khalique Ahmad [a], Faisal Hossain [b]

[a] Graduate Student, Dept. of Civil and Environmental Engineering, Univ. of Washington, More Hall 201, Seattle, WA 98195.

[b] Professor, Dept. of Civil and Environmental Engineering, Univ. of Washington, More Hall 201, Seattle, WA 98195 (corresponding author). E-mail: fhossain@uw.edu; Phone: (931) 239 4665

Abstract

This study explores the maximization of hydropower generation by optimizing reservoir operations based on short-term inflow forecasts derived from publicly available numerical `weather prediction (NWP) models. Forecast fields from the NWP model of the Global Forecast System (GFS) were used to force the Variable Infiltration Capacity (VIC) hydrologic model to forecast reservoir inflow for 1-16 days lead time. A reservoir operations optimization strategy was applied based on the forecast of inflow. The concept was demonstrated for two dams in the United States. Results showed that a significantly greater amount additional hydroelectric energy benefit can be derived consistently than the traditional operations without optimization and weather forecasts. Goals of flood control and dam safety also were not compromised when exploring opportunities for hydropower maximization. The study clearly underscores the additional value of weather forecasts that are available publicly and globally from NWP models for any dam location for hydropower maximization. Given the on-going effort to coordinate strategies for sustainable energy production from renewable energy sources, it is timely that this concept be expanded further to current hydropower dam sites around the world. This can help reduce dependence on

fossil-fuel based energy production and shift towards greener sources using existing hydropower infrastructure.

Keywords: hydropower, maximization, short-term weather forecasts, reservoir operations optimization, flood control.

1. Introduction

Improving production from renewable energy sources is required in reducing the dependence on fossil fuels and addressing the global energy security in a sustainable way. As envisioned by [1], unless a replacement energy infrastructure is developed well ahead of time, economic, social and political instability may ensue due to heavy fluctuation in the supplies and price of fossil-fuel [2]. The renewable sources of energy are not subject to such price fluctuations as they come from the available natural sources of water, sunlight, wind, tides etc. [3]. A recent study concluded that the use of wind, solar, hydroelectric, tidal and geothermal energy is the most beneficial, among several other alternatives, for addressing pollution, public health, global warming, and energy security [4].

The use of wind, water and sunlight to suffice for the electricity demands within U.S. as well as worldwide has been explored by [1,5-7]. Some of these studies have projected the future renewable energy potential to lie exclusively in the variable sources of wind and solar power and claimed them to be sufficient to meet the energy demand [8-11]. However, hydropower remains a key renewable source to generate the baseload power (minimum power needed at a steady rate) due to its relatively high capacity factor [12] and minimal potential interruptions to the system [13,14]. Factors that further necessitate studying hydropower systems include its significant operational flexibility with ability to store energy [15], instant power generation [16], low operating and maintenance costs [13], and capability of integration with intermittent renewables [15,17,18]. This is manifested in recent effort of wind-hydro combination projects by the German firm *Max Bögl* [19].

Within the U.S., over the past 65 years (1950-2015), hydropower has contributed 10% to the total and 85% to the renewable power generation [19]. However, the installation of newer hydropower capacity has declined in the past couple of decades. According to the U.S. Department of Energy [19], the amount of nation’s net electricity generation contributed by hydropower has decreased, from 30% in 1950 to 7% in 2013, as nuclear power, coal, natural gas, and other sources were added to the nation’s energy portfolio to meet rising demands. In the last decade, no large-scale hydropower dam project, exceeding 500 megawatts (MW), has been constructed in the U.S. due to factors such as lower economic growth, concerns related to environmental impacts, stagnant energy market, and uncertainties owing to the recent breakthroughs in the shale gas and oil industries [20]. Fig. 1 illustrates this stagnation observed in the growth of hydropower capacity after 1990. Further, as most economical hydropower sites in U.S. have already been explored over the previous century, any rise in the hydropower infrastructure is hardly expected [21]. Given that we are no longer building new hydropower dams in the developed world such as the U.S., it is worthwhile to explore how existing infrastructure can be maximized of its operational effectiveness to provide more power to the energy grid by optimizing the operations [22].

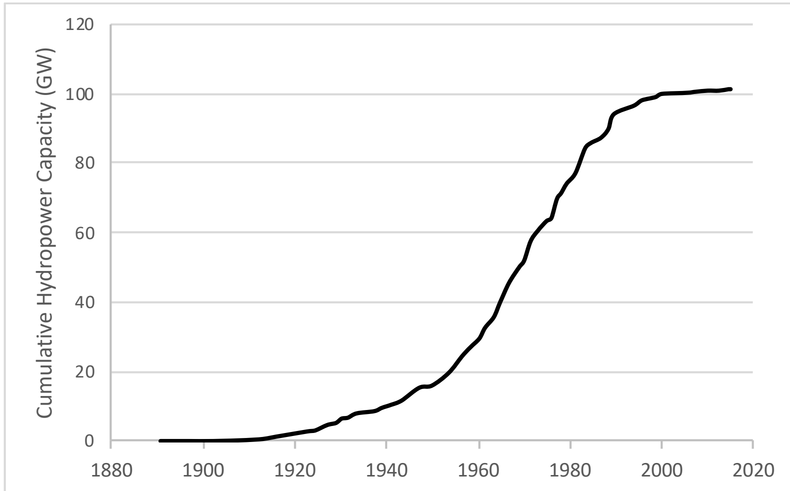

Fig. 1. Cumulative installed hydropower capacity from 1890-2015 over the United States (Reproduced from [2])

The current management of most federal reservoirs at daily time scale is based on rule curves that outline the reservoir storage targets to be met at specific time intervals of the year. The rule curves were designed based on existing storage volumes using a climatology of historical flow observations [23, 24]. Operating strictly based on these rules, without considering the altered demands or changes in inflow patterns [71, 72] can cause mishandling of an impending and unexpected reservoir inflow situation at the weather scale. Such a situation can lead to missed hydroelectric energy [20]. For example, in a weaker-than-average month of the flood season, lowering the pool to rule curve level too early can result in significant loss in power generation, which could be avoided if the inflow forecasts are made ahead of time. Thus, it is timely to leverage the advancements in atmospheric modeling for forecasting the weather [25] and optimization techniques to achieve the goal of maximizing hydropower energy and realize more efficient and 'smart' reservoir operations management.

The NWP weather models from various meteorological agencies produce weather scale forecasts fields of precipitation, temperatures, wind speed, soil moisture etc. in three dimensions over the entire globe. These publicly available forecasts represent an underutilized low-hanging fruit for the hydropower community. Currently, the integration of such forecasts into existing water management decision processes at weather scale is not yet popular or mainstream due to the traditional risk averse nature of water managers. The major concerns include low forecast skill and mismatch in the scales of forecasts from those required by the stakeholders [13,22,26,27]. However, a recent study has concluded that the forecast skill of NWP models at a lead time of 7 days has improved from 50% in 1995 to more than 70% in 2015 [15]. Such an improvement can capture the peaks of a flood event and can be utilized to adjust the dam operations accordingly. Reservoirs in the snow-dominated regions like the west coast (e.g. Columbia River basin) frequently use seasonal projections of climate, snowpack forecast etc. to optimize their operations [13,27]. Ongoing projects such as Integrated Forecast and Reservoir Management (INFORM) [28] and Forecast Informed Reservoir Operations [29], that have focused over specific watersheds, are also utilizing short-term weather forecasts for operating the reservoirs. Another issue is the coarse resolution of the NWP forecast fields that are often not detailed enough to be applied over the relatively small reservoir catchments. To address this, dynamic downscaling technique can be used to resolve the atmospheric processes at finer scale [30-32]. To the best of our knowledge, there has not been any study to explore the value of dynamically downscaled NWP based-forecasts specifically for hydropower maximization.

To utilize the forecast inflow information for generating more energy, the reservoir system needs an optimal and more informed set of release decisions updated dynamically based on the current reservoir state and future inflow. Various optimization techniques have been proposed in the past, and an extensive literature review and evaluation of different state-of-the-art approaches can be found in [21,33-35]. The optimization objective is the key towards optimizing operations as there are a plenty of studies focusing on single user benefits. These include optimizations for hydropower production [36-38], flood control and security [23,39,40], water supply [41,42], irrigation and crop planning [43,44] and environmental concerns [20]. However, due to the wide-ranging diversity of property rights and stakeholders, optimizing for a single stakeholder is ill-advised, rather the competing purposes (such as flood control and irrigation) needs to be balanced for extracting equitable benefits out of the existing infrastructure. In several multi-objective optimization studies [45-52], the focus has been on the dams with significantly large reservoir storage capacity. Short-term forecasts, as used here, are likely more valuable for the dams with reservoir capacity smaller than the annual inflow volume [27]. This study specifically explores such dams, usually unaddressed in the existing literature, for hydropower operations incorporating the weather-scale forecasts.

The overarching research question addressed here is – *can the short-term weather forecasts from numerical weather prediction improve the hydroelectric energy production for small and medium storage dams without compromising flood security, dam safety and environmental flow constraints?* A schematic of the approach highlighting the major components of the study is shown in Fig. 2 and is explained in the following sections.

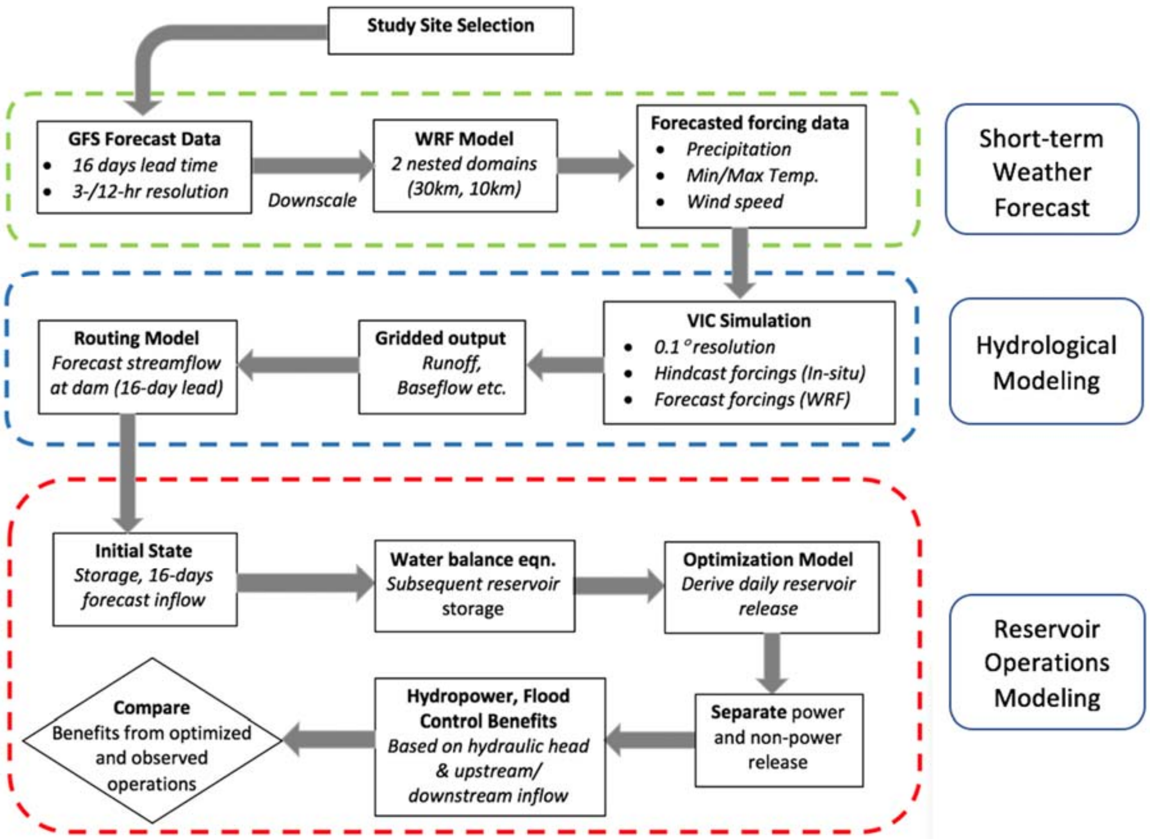

Fig. 2. Illustration of the approach used in this study. Green box – forecasting; Blue box – hydrologic modeling; Red box – optimization component. VIC is the hydrologic model for predicting inflows. GFS is NOAA's Global Forecasting System for weather forecasts.

2. Material and Methods

2.1 Study Region and Data

An exploration was made for dams satisfying the following criteria: (i) operated for hydropower generation or flood control as their primary or secondary purpose, (ii) have reservoir storage capacity less than a threshold of 1,700,000 ac-ft (98th percentile value for reservoir storage within U.S., see Fig. 3), (iii) located upstream in the dam network (in case of a multi-reservoir system) to receive unregulated inflow, to facilitate hydrological modeling, and (iv) reservoir storage capacity smaller than annual inflow volume for the short-term forecasts to be valuable [27]. Out of the several potential locations, Detroit dam in Oregon and Pensacola dam in Oklahoma, were selected based on the data availability and processing time constraints. Both the Detroit dam, located at the North Santiam River forming Detroit Lake, and Pensacola dam on the Neosho River forming Grand Lake are primarily used for hydropower and flood control. The powerhouse at Detroit dam contains two Francis turbine units with a combined nameplate capacity of 100MW, while Pensacola dam, Oklahoma's first hydroelectric power plant, consists of six turbine generator units with the nameplate capacity of 120MW. The observed streamflow data was obtained from the U.S. Army Corps of Engineers (USACE) [53,54]. The reservoir storage capacity and ratio with annual inflows are shown in Table 1 and locations of the selected dams in Fig. 4.

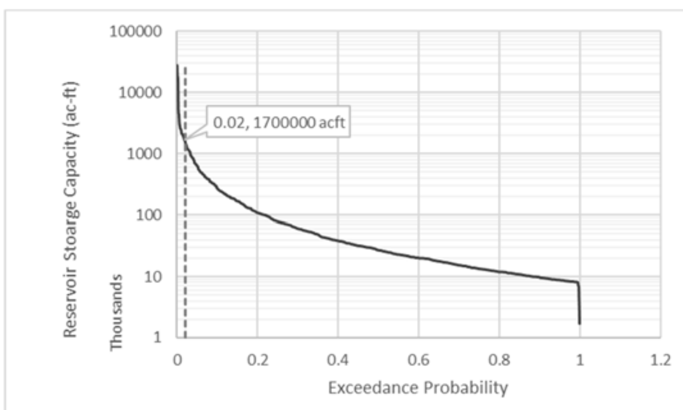

Fig. 3. Distribution of the storage capacity of dams in U.S. Data obtained from Global Reservoir and Dam (GRanD) database [73].

Table 1. Comparison of Storage Capacity and Annual Inflow for the two dams

Dam	Storage Capacity (ac-ft)	Annual Inflow (ac-ft)	Capacity-Annual Inflow Ratio
Detroit	455,000	1,420,360	0.32
Pensacola	1,672,000	5,996,482	0.28

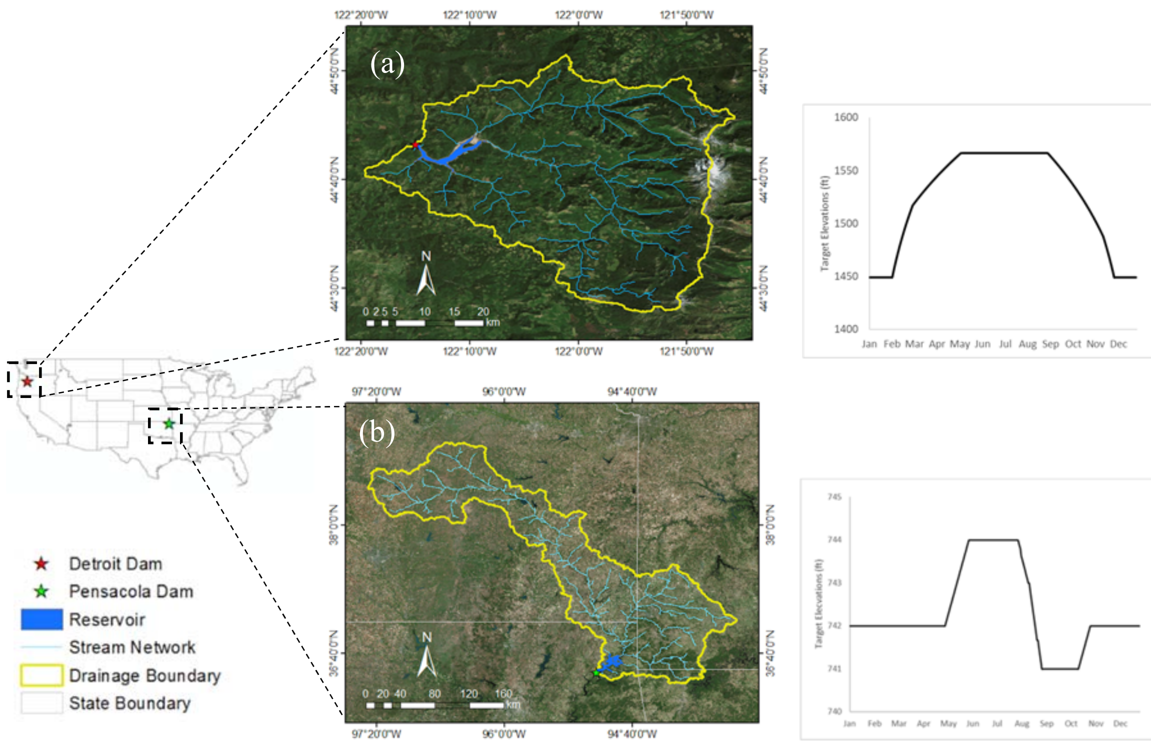

Fig. 4. Location, drainage boundaries, stream networks on the left panel and rule curves for (a) Detroit Dam, OR; (b) Pensacola Dam, OK, on the right panel.

2.2 Short-term NWP based forecasts

Real-time short-term (1-16 days) forecast data from the Global Forecast System (GFS) global-scale NWP model was acquired at 0.5˚ resolution. The global forecasts are produced four times a day for 1-16 days lead time in almost real-time by National Centers for Environmental Prediction (NCEP) [76]. Dynamic downscaling was performed using the numerical Weather Research Forecasting (WRF) model to output forecasts at 0.1˚ resolution. WRF, a mesoscale atmospheric numerical modeling system, has demonstrated its capability for constructing the atmospheric conditions, at both local and regional scales [55,56]. Two nested domains of 10 km and 30 km were used for the dams as shown in Fig. 5**Error! Reference source not found.**.

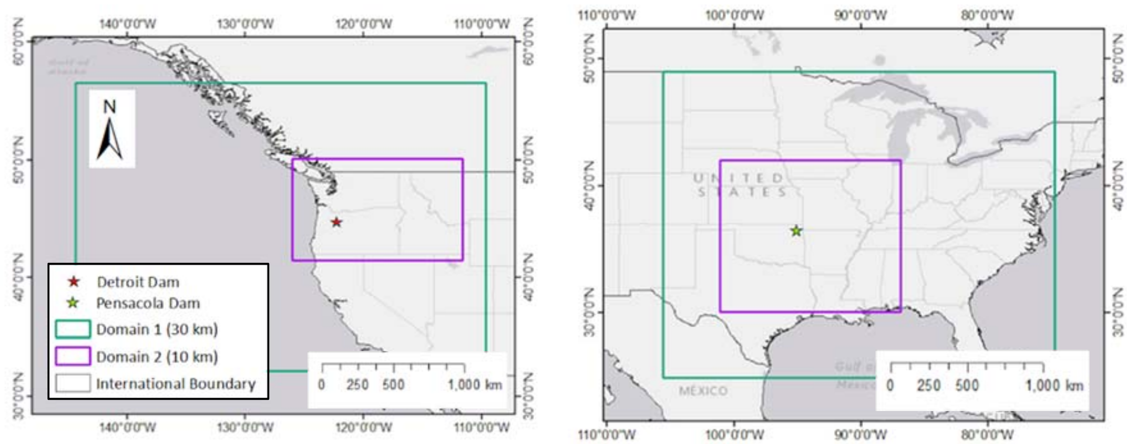

(a) (b)

Fig. 5. The nested domains for WRF simulation at 30km and 10km, for (a) Detroit Dam, OR and (b) Pensacola Dam, OK.

In a numerical model like WRF, the Microphysics (MP) and Cumulus Parameterization (CP) schemes are the controlling factors for precipitation as reported in existing literature [57, 55]. As the Detroit dam lies in the Pacific Northwest region, the model configurations were inherited from the forecast model runs of Department of Atmospheric Sciences at the University of Washington [58]. The Thompson graupel scheme was considered for MP and Grell-Devenyi ensemble scheme for CP. For Pensacola dam, the Morrison microphysics scheme was used as recommended by [55] for extreme storm simulations. Appendix A evaluates the performance of WRF setup for both the dams.

2.3 Hydrologic Model

The macroscale semi-distributed Variable Infiltration Capacity (VIC) hydrologic model [59, 60] was chosen to model the reservoir inflow. The VIC model is forced with the time series of gridded precipitation, minimum and maximum temperature, and wind speed. The macroscale model was run at a daily time scale at 0.1° spatial resolution to ensure that the basin contains enough grid cells for simulation. The hindcast forcings were obtained from NCDC Global Surface Summary of the Day data [61] while the WRF-downscaled GFS fields provided the forecast forcings for the VIC model. To obtain the inflow at the downstream station of basin, routing of streamflow was performed separately using the routing model of Lohmann et al. [62,63]. Model calibration was performed by adjusting the parameters of VIC model that govern baseflow recession, infiltration, and soil layer depths to match the simulated streamflow with reference data, minimizing the root mean squared error (RMSE). The calibration and validation details of VIC model are provided in Appendix B.

2.4 Reservoir Operations Model

The next step (Fig. 2, red box) is to model the reservoir operations using the forecast inflow information optimizing the releases from the reservoir to maximize hydropower generation. Optimizing at the daily time step is most suitable when it comes to real-time operations of small and medium-storage dams. A small dam operator is very unlikely to be making decisions on reservoir releases for such dams at frequencies higher than a day.

2.4.1 Optimization Strategy

In general, setting up the reservoir's optimization framework involves three components – 1) advanced scheduling of water releases, 2) useful inflow forecasts that serve as input data, and 3) and optimization model that utilizes forecast information to the best advantage [33]. A major limitation in operating the reservoirs occurs during the flood/peak flow seasons when the high uncertainty in predicting a flood peak leaves the dam operator uncertain on much water to release to balance the various stakeholder benefits. The short-term forecast information was utilized here to provide the operator with a release policy optimized to simultaneously maximize benefits from the conflicting objectives.

To minimize the effect of reduced forecast skill with increasing lead times (see Appendix A), the optimization strategy sequentially updates NWP-based (downscaled by WRF) flow forecasts every other day. Evaluation is performed by calculating optimized hydropower benefits (*optimized* HP) using the optimized releases while passing the observed inflow into the system. The *optimized HP* benefits were compared against the observed benefits (*observed HP*) using observed operations without any optimization/forecasts. The observed benefits correspond to the real-world power generation data obtained from USACE that operates the two dams. The optimized hydropower benefits (megawatt-hours, MWh) were calculated as a product of hydraulic head and power release (via penstocks), considering the turbine efficiency, operating hours and the capacity factor (ratio of actual hydropower produced to the maximum possible over a period).

2.4.2. Optimization Objectives and Constraints

Reservoir operations were formulated as a Multi-objective Optimization Problem (MOP) based on a Pareto optimal set of solutions with the objective functions of hydropower maximization and flood control [64]. The two objectives are mutually conflicting, since maximizing hydropower production requires higher reservoir storage to produce more power, while for minimization of the flood risk, more water needs to be released to ensure enough storage when the peak inflow hits the reservoir. The Non-dominated Sorting Genetic Algorithm (NSGA-II) [65] was used to yield the Pareto front of the optimal solutions from which an appropriate alternative can be chosen at various satisfaction levels of both the objectives [66]. The two conflicting objectives are formulated below.

1. Minimize the deficit in hydroelectric power production (MW) from the maximum generation capacity of the powerplant (HP_{max}),

$$\min f_1(MW) = HP_{max} - \sum_t \epsilon \cdot \Delta t_{turb} \cdot (HF_t - HT_t) \cdot R_{p,t} \qquad (1)$$

2. Minimize the absolute value of deviations of reservoir elevation (H) from the target rule curve level (T) over the optimization horizon. It is represented as,

$$\min f_2(ft) = \sum_t |H_t - T_t| \qquad (2)$$

$t -$ 1-16 days (optimization horizon)

HF – Reservoir forebay water level (ft)

HT – Reservoir tailrace water level (ft)

ϵ – Turbine efficiency

Δt_{turb} – Turbine operating hours

$R_p -$ Power release from turbines (cfs)

Several constraints were imposed on the optimization problem in the interest of downstream stakeholders, dam safety and environmental concerns. The power and spillway release from the reservoir were limited by the turbine and spillway capacity. The minimum for reservoir storage was set to 95% of the historical minimum and the maximum to the flood control pool while following the storage-volume continuity. The total release was bounded between the environmental flow limit and a safe threshold to prevent flooding at a downstream control station. The mathematical formulation of the constraints is given in Appendix C.

3. Results

Three case studies are presented for forecast-based hydropower maximization using optimized reservoir operations. Two of them were performed over a single storm flow event each for Detroit and Pensacola dams, while a third long-term assessment was performed over a continuous period of ten months for Detroit dam with a long dry spell.

3.1 Detroit Dam – Single Event Assessment

The various pools of the reservoir along with the constraints used in setting up the optimization model are shown schematically in Fig. 6. The maximum total release was set to control the downstream point of Mehama to a threshold of 9000 cfs to prevent downstream flooding.

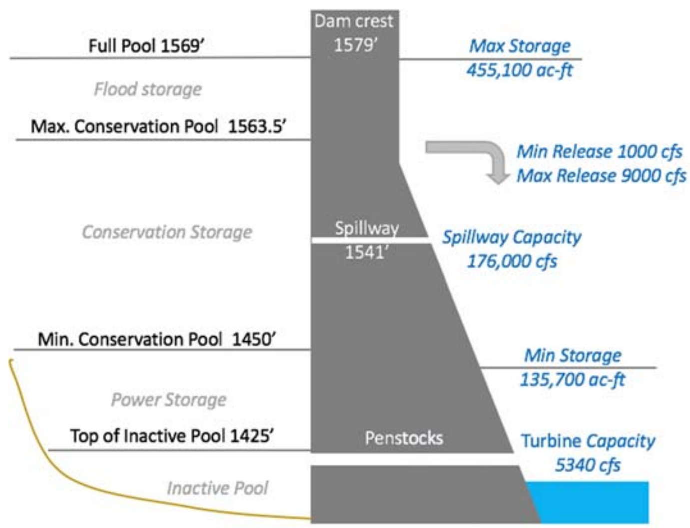

Fig. 6. Cross-section of Detroit dam (not to scale) showing relevant pool elevations (from mean sea level, MSL) along with the optimization constraints obtained from USACE.

The flow event of 21 Dec 2014 with peak inflow of 24,170 cfs (yearly-scale magnitude) was selected. As the turbine operating characteristics vary over an event or a season, model for hydropower estimation (MWh) based on available daily energy generation data (MW) was developed. Linear regression was performed between the energy generation (in MWh) and the product of hydraulic head ΔH and power release R_p to obtain an average estimate of 19.72 hours for turbine's operating hours coupled with its efficiency (the constant $\epsilon \cdot \Delta t_{turb}$ in Eq. (1)).

The 16-day forecast inflow obtained using the VIC model forced with WRF-downscaled forecasts for lead times of 3, 5 and 9-days over the selected event are shown in Fig. 7(a).

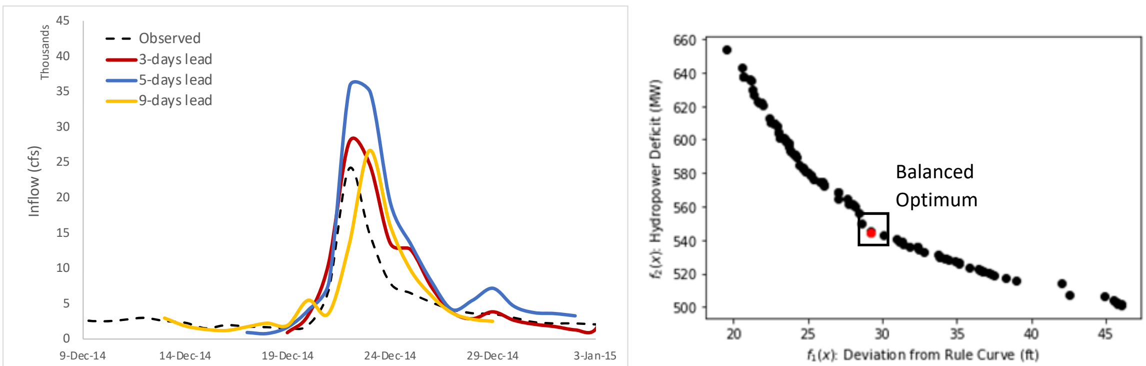

(a) (b)

Fig. 7. (a) VIC-modeled 16-day forecast flow forced with WRF-downscaled forecast fields, for lead times of 3, 5 and 9 days; (b) Non-dominated solutions on the Pareto front and the selected balanced optimum obtained between the objectives of hydropower deficit and deviation from rule curve (to be minimized). Detroit dam, OR.

The optimized release policy was obtained with the optimization starting on Dec 11. A set of 100 non-dominated points on the tradeoff curve (Pareto front) obtained between the two competing objectives are shown in Fig. 7(b) for the first day of optimization. A balanced optimum solution was chosen on the Pareto front giving equal priority for hydropower deficit and flood risk (in terms of deviation from rule curve) and aiming at concurrently minimizing both the objectives. The conflicting nature of the two objectives can be clearly observed from the shape of the Pareto curve.

The optimal release of first two days were implemented while the later ones were revised in the next model run on Dec 13 using updated forecasts. The sequential updating of forecasts was continued every alternate day until Dec 19. This resulted in the optimized release as shown in Fig. 8 (a). While the releases and elevations from Dec 11-19 are obtained by sequentially updating the forecasts, the values afterwards are obtained from the last optimization run of Dec 19.

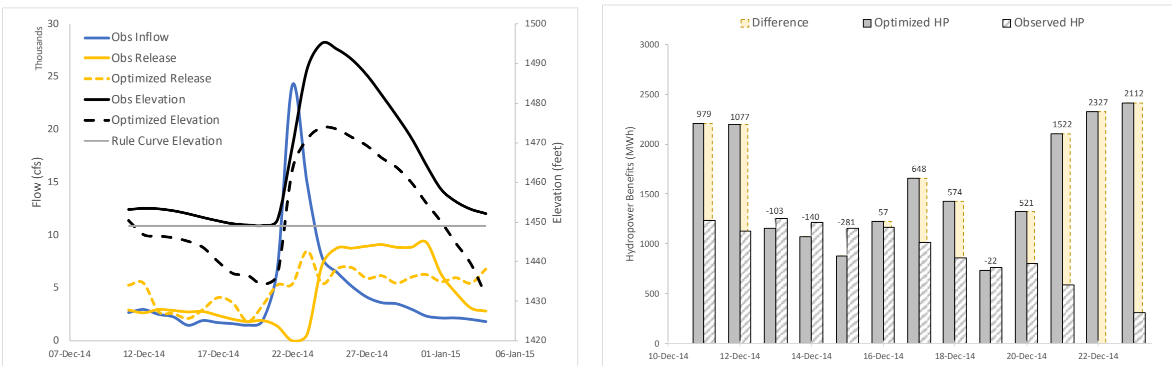

(a) (b)

Fig. 8. (a) Optimized releases and elevations from the sequentially updated forecasts from Dec 11-19, along with the respective observed values, (b) Daily comparison of hydropower benefits (MWh) from optimized and observed operations (Detroit dam, OR). 'HP' stands for Hydropower; yellow bars and labels show the difference in benefits from the two set of operations.

As can be seen from Fig. 8(a), the optimized operations result in a higher release as soon as the peak inflow is forecasted due to which the reservoir levels (black dashed curve) drop down within dam's safety limits, and then surges as the peak hits the reservoir. The elevation at the end of the optimization period, however, has a slightly higher deviation from the rule curve (compared to the observed value) as the sequential updates to forecasts have only been made till Dec 19. An *optimized hydropower benefit* of 20,720 MWh was obtained in comparison to the observed production of 11,450 MWh over Dec 11-23. Thus, an additional benefit of 9,270 MWh of hydropower could have been generated before and during the peak inflow event based on weather forecasts and optimization. The daily comparison of hydropower benefits from the optimized and observed operations is shown in Fig. 8(b).

3.2 Pensacola Dam – Single Event Assessment

Similar to Detroit dam, we identified the dam's relevant pools, the operating constraints and turbine features, as depicted in Fig. 9. The optimization constraints for Pensacola dam were obtained from USACE. For the maximum total release, the threshold of 30,000 cfs was selected as a flood-safe value of streamflow at the downstream USGS gage of Neosho River (site ID - 07190500) while the minimum value was selected to allow a safe environmental flow of 1000 cfs based on the historical observed release data.

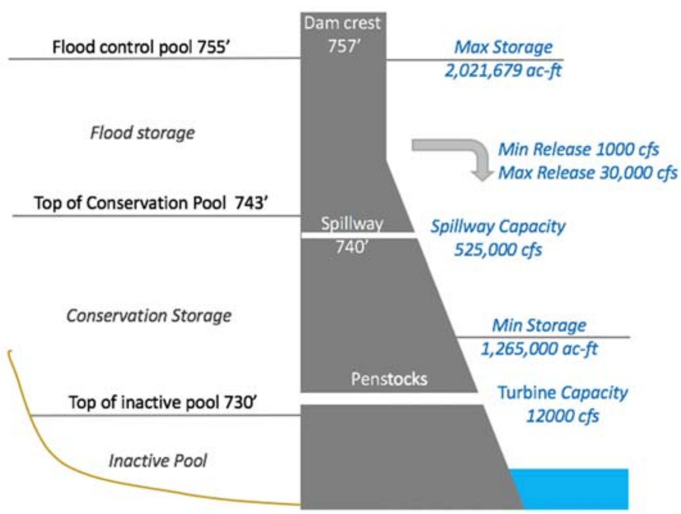

Fig. 9. Cross-section of Pensacola dam (not to scale) showing relevant elevations (from mean sea level, MSL) and the selected constraint values obtained from USACE.

The inflow event of 22 Mar 2012 with a peak flow of 82,350 cfs was chosen for Pensacola dam. As the actual hydropower data (MWh) is not provided on USACE data portal, an estimate of turbine's operating hours and efficiency could not be obtained. Hence, a value, close to that for Detroit, of 20 hours was chosen for the constant in hydropower equation ($\epsilon \cdot \Delta t_{turb}$) (Eq. 1), as both the dams have similar installed hydropower capacities. The 16-day forecast inflow modeled for lead times of 3, 5 and 9-days is shown in Fig. 10(a).

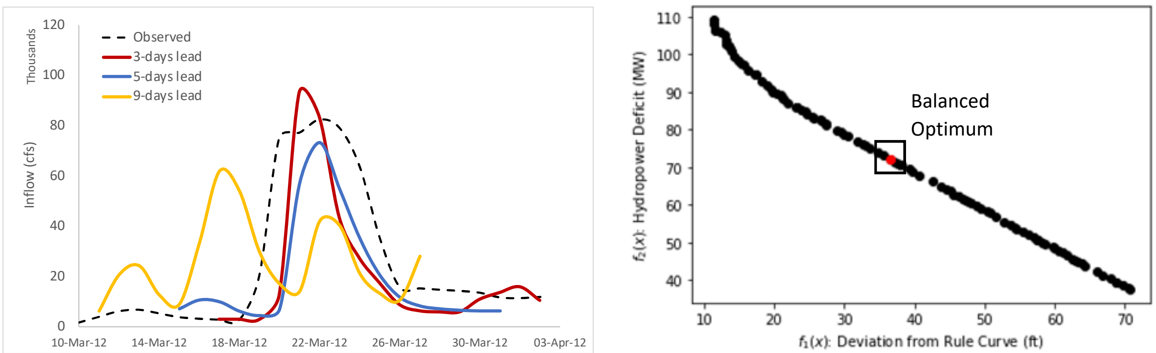

(a) (b)

Fig. 10. (a) VIC-modeled 16-day forecast flow, forced with WRF-downscaled forecast fields, for lead times of 3, 5 and 9 days; (b) Pareto front and the selected balanced optimum obtained between the two objectives, Pensacola dam, OK.

The Pareto front with the non-dominated solutions and the chosen balanced optimum is shown in Fig. 10(b). The optimization based on sequential updates to WRF forecasts for this dam revealed *optimized hydropower benefit* of 31,650 MWh from Mar 11-24, as compared to the *observed benefit* of 18,825 MWh. Again, an additional production of 12,825 MWh pre- and over the peak flow event was realized. The optimized releases and reservoir elevations are compared with the respective observed values in Fig. 11(a) and the daily hydropower benefits plotted in Fig. 11(b).

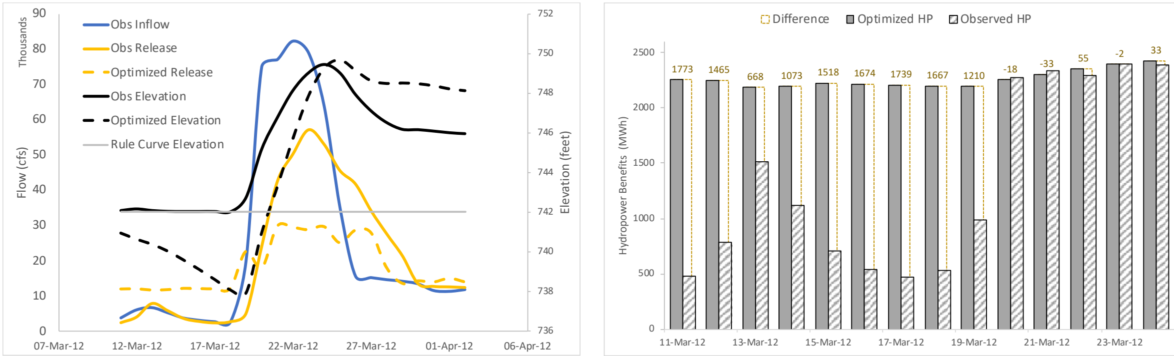

(a) (b)

Fig. 11. (a) Optimized releases and elevations updating forecasts every alternate day from March 11-17, with the respective observed values; (b) Daily comparison of hydropower benefits (MWh) obtained using observed and optimized operations (Pensacola dam, OK). 'HP' stands for Hydropower; yellow bars and labels show the difference in benefits from the two set of operations.

3.3 Long-term Assessment of Hydropower Benefit

To put our concept to test in the practical world, the reservoir operations model for hydropower maximization using WRF-downscaled forecasts were automated through an online decision support system (see http://depts.washington.edu/saswe/damdss) for Detroit dam. The long-term results obtained from Dec 2017 to Sep 2018 (10 months), consist of both wet and dry seasons. A 16-day optimized operation schedule was derived using the WRF model's downscaled GFS forecasts. Using the actual inflow that occurred during the day and the respective optimized releases, final reservoir storage was computed by satisfying the storage-volume continuity (see Appendix C). The final storage of the first day served as the next day's beginning storage to obtain the next set of optimized releases using the updated forecasts. The model was run for all the ten months using such daily sequential updates. A similar update process was followed by [75] at a weekly scale.

The hydropower benefits from the optimized operations are compared with the observed power generation data from USACE in Fig. 12, plotted together with the respective inflow and release. The plots suggest that during the peak flow seasons, optimized policy results in higher release ahead of the event leading to higher energy generation. For low flows, the optimized release is constrained by the environmental flow limit of 1000 cfs, although the actual operations go below this limit on a few days. The total optimized hydroelectric energy (*optimized HP*) of 258,120 MWh was obtained over the 10-month period in comparison to the observed benefit (*observed HP*) of 244,490 MWh. Thus, an additional hydropower benefit of 13,630 MWh (optimized minus observed hydropower) was obtained over the longer term that included both wet and dry seasons. The highest benefits in energy were obtained when a peak inflow occurs, as that is when the dam operator is most uncertain on the release to be made often leading to 'missed hydropower.' There are also episodes when the energy generation from observed operations exceeded the optimized ones (red bands in Fig. 12) that occur during the low flow periods, generally after a peak inflow event. Also, the assumption of constant turbine's operating hours and efficiency might not hold true, due to change in its efficiency or future addition of more turbines. However, the optimized release policy did not compromise the other objectives (of flood control and dam safety) by not exceeding the safe threshold of downstream flooding and satisfying the environmental flow constraints. Overall, in a longer period, the concept has potential in producing more energy benefits, overcoming the concerns of false alarms and false low flows, when operationalized in real-time operations over the existing infrastructure.

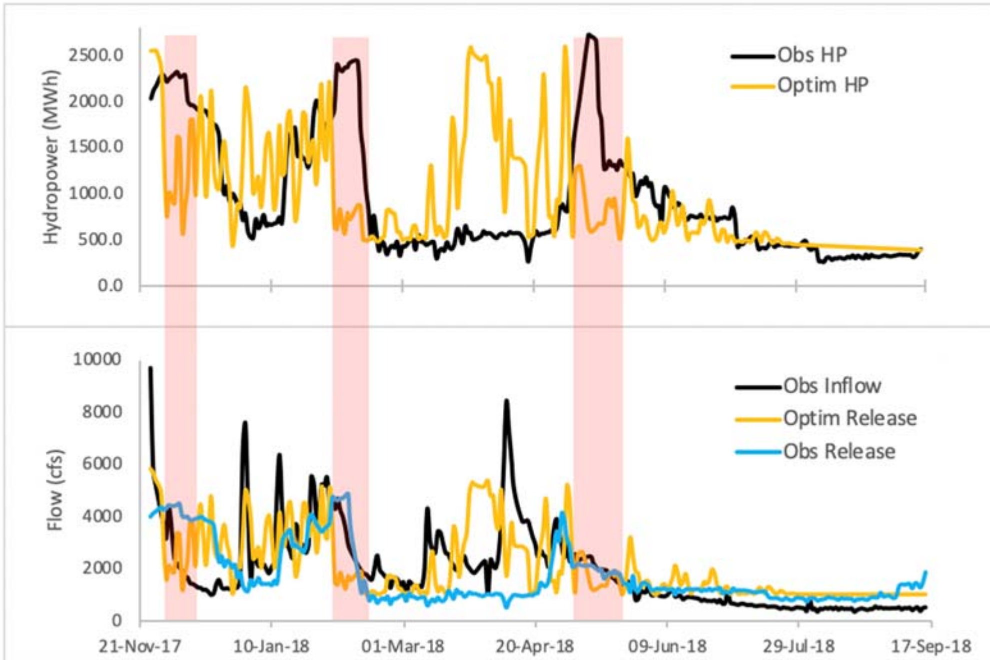

Fig. 12. Optimized hydropower benefits obtained by sequentially updating forecasts every day, compared with the observed benefits (top); optimized and observed release policy compared along with the observed inflow (bottom). Red bands highlight the days when optimized power was exceeded by the observed power generation.

4. Discussion

4.1 Performance Assessment - Hydropower versus Flood Control benefits

In order for the proposed optimization strategy to be effective, the two competing objectives of hydropower and flood control need to be satisfied simultaneously. For the Pensacola dam, during the Mar 2012 peak event, the proposed optimization strategy was able to generate an additional 12,825 MWh of energy on top of the production from observed operations. This amounts to a revenue of $1,251,720 using the average residential electricity rate of 9.76¢/kWh in Oklahoma City [67]. At an average electricity consumption of 900 kWh per month per US household, this additional energy can fulfill the demands of around 11,545 more households for one month. For the competing flood control objective, the performance was assessed from the reduction in the outflow peak over the event. For the selected event, a maximum observed release of 57,211 cfs was limited to just 30,000 cfs (47.5% reduction) as a safe threshold to prevent flooding downstream.

For Detroit dam's single event assessment, the proposed optimized operations were able to generate an additional 9,270 MWh of hydropower (on top of the observed value). Again, this energy equivalent to revenue of $908,460 at a rate of 9.8¢/kWh in Oregon [68] that can power up to 8,345 US households for a month. For the long-term assessment over ten months (with inflows lower than the considered individual peak events), the additional energy amounted to 13,630 MWh and the optimization strategy was most effective during the high inflow periods. The reservoir release was kept under the flood-safe limit of 9000 cfs for the downstream control station. Thus, the proposed optimization strategy not only generates more hydroelectric power but also addresses the other key objective of reducing the flood risk.

The two dams for the case study assessments were chosen in different hydrological regimes with varying characteristics. As the Detroit dam lies in with steep terrain with small sized basin and fast hydrological response, the rainfall quickly gets converted into runoff with a lesser time of concentration. However, Pensacola dam possesses a flatter terrain with longer rivers resulting in higher time of concentration. Thus, the successful assessment over both the dams, over individual high inflow events as well as operationally over longer term, illustrates the robustness of the concept.

4.2. Scalability of Hydropower Maximization

While the dams selected for study have different hydrologic regimes, catchment characteristics and reservoir inflows, the variation is certainly much higher across the dams over U.S. and the globe. This variation cannot be captured by the analysis presented in this study. However, the practitioners are encouraged to study and extend the framework of optimization to improve the hydropower generation scenario using weather forecast information over other dams suitable for such kind of exploration. These include the dams that are (a) powered, (b) have small to medium reservoir storage capacity, and (c) upstream in the dam network receiving unregulated flow. An analysis over the U.S. dams revealed 525 dams satisfying these criteria, amounting to 23% of the 2248 powered dams [69]. These dams are shown in Fig. 13 and are the sites for further exploration of their suitability for the concept. We believe that the concept, if extended to a good fraction of such dams, has the potential to bring the nation closer to an energy infrastructure independent of the fossil fuels and other non-renewable sources.

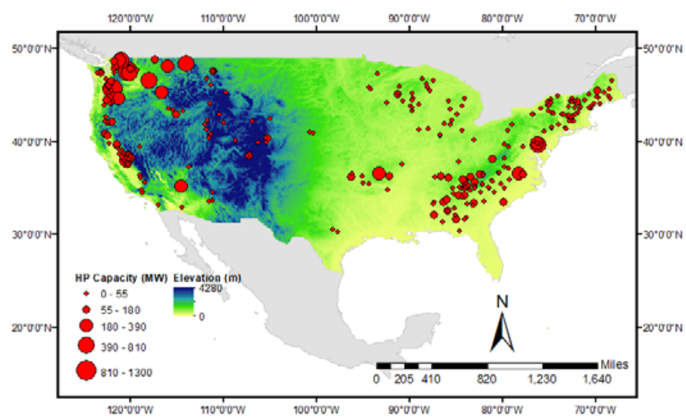

Fig. 13. Locations of upstream dams receiving unregulated inflow to be explored of their suitability for weather forecast use in optimizing reservoir operations.

5. Conclusions

The purpose of this study was to evaluate the potential of short-term weather forecasts to extract more hydroelectric energy, without compromising other competing objectives. The NWP model-based weather forecasts, their dynamic downscaling, hydrologic modeling, and the optimization algorithm were coupled with reservoir operations model to obtain the optimized release policy for maximizing energy production. The concept was demonstrated over two dam sites with varying hydrological characteristics receiving unregulated inflow. Performance assessment over two year return period storm events and a longer ten-month period (of wet and dry seasons), showed significant energy benefits that could be reaped over the long-term. The optimization not only improved the energy production, but also helped achieve the goals of flood control and dam safety. The Pareto optimality allowed the operator to choose an appropriate optimal solution depending on the prevailing circumstances in operating the reservoir. It should be noted that, at least for the type of dams demonstrated here, the forecasts help the most during the peak flow (wet) period when uncertainty in the reservoir inflow is high causing over-conservative operations. Nevertheless, the long-term benefits of maximizing the hydropower every day, even in small amounts, is a low-hanging fruit that should not be overlooked, rather be explored to its depth to realize a more sustainable framework for reducing the dependence on fossil-fuel based energy generation. Future research needs to include integrating the power demand forecasting with the reservoir operations model so that the opportunity to generate additional power is not missed during times of peak demand.

Combining optimization and simulation models for managing water resources in a real-world setting has not been fully realized yet [74]. By using real data on real dams with real-world constraints, we have demonstrated very clearly that the currently available weather forecasts from NWP models have a lot to offer to address energy security. Thanks to the advances in atmospheric science and modeling, these weather forecasts are already available publicly. The challenge now is to convert availability to accessibility so that dam operators can operate based on an improved advisory that makes hydropower generation more efficient (more power with same or less impounded water) and reduce our impact on the natural world.

Appendix A. WRF performance evaluation

The evaluation of dynamically downscaled forcings of precipitation, min/max temperature and wind speed from WRF was performed using Livneh daily CONUS near-surface gridded meteorological dataset [70]. For Detroit dam, due to the absence of Livneh dataset after 2014, WRF model evaluation was performed for the peak flow event of 16 January 2011. The GFS forecasts for 3, 5 and 7-days lead time were downscaled using WRF. In the case of Pensacola dam, WRF model was set up for the peak inflow event of 20 March 2012 and forecast data corresponding to lead times of 4, 6 and 8-days was processed for downscaling. The metrics of correlation, RMSE, Probability of detection (POD) and Frequency Bias [55] were calculated to assess the performance with different lead times. POD is the measure of how well the simulation can capture the true positives while frequency bias measures the extent to which the simulated results are biased towards false positive/negative (both having best value of 1). For both dams, performance of the forecast model deteriorates with lead time, with higher number of misses (true negatives) and false positives. The comparison maps of precipitation are shown in Fig. A.1 for the selected peak flow events and Table A.1 summarizes metrics for both the dams.

Table A.1. Metrics for evaluation of WRF downscaled forcings for lead times of 3-8 days (L3-L8).

Variable	Metric	Detroit Dam			Pensacola Dam		
		L3	L5	L7	L4	L6	L8
Precipitation	Correlation	0.85	0.84	0.19	0.61	0.31	-0.09
	RMSE (mm)	11.18	21.62	15.86	23.39	30.52	33.57
	POD	0.93	0.96	0.04	0.72	0.66	0.57
	Freq. Bias	2.28	2.56	0.04	0.76	0.67	0.58
Max. Temperature	Correlation	0.53	0.48	0.48	0.78	0.71	0.64
	RMSE (˚C)	4.88	4.65	6.05	3.73	4.82	5.19
Min. Temperature	Correlation	0.68	0.67	0.68	0.87	0.82	0.58
	RMSE (˚C)	5.45	5.34	3.46	2.07	2.26	3.23
Wind Speed	Correlation	0.16	0.36	0.01	0.61	0.45	-0.19
	RMSE (m/s)	2.26	2.03	2.56	1.70	1.88	2.76

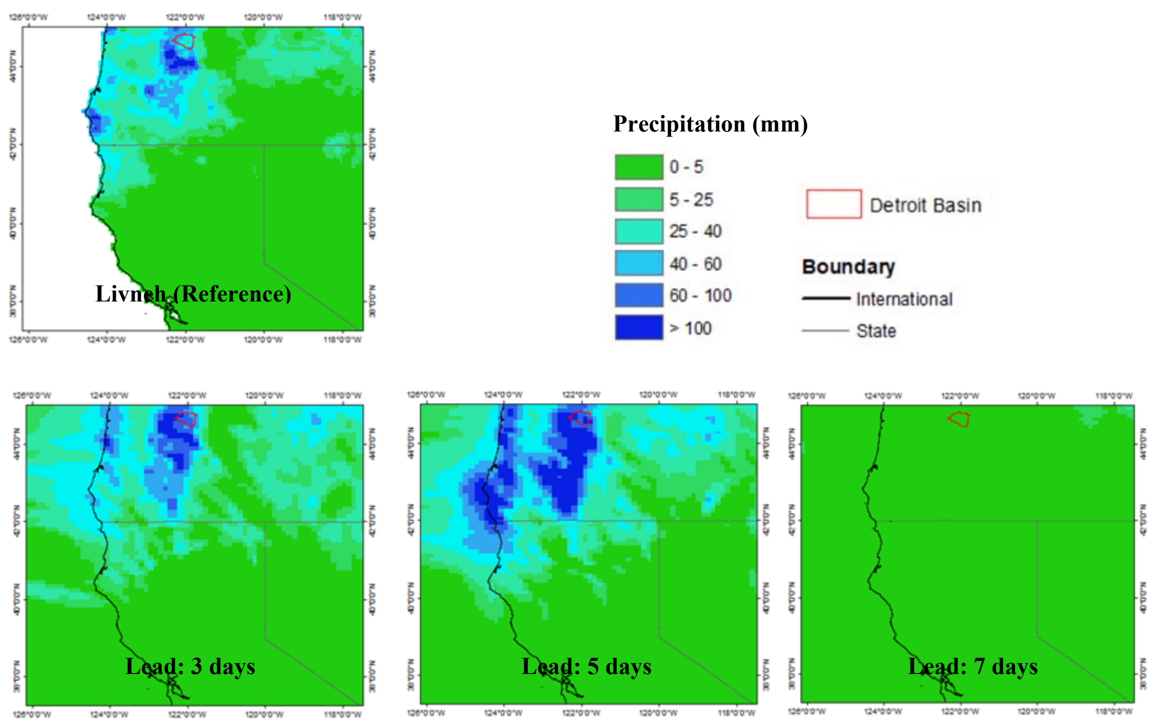

(a)

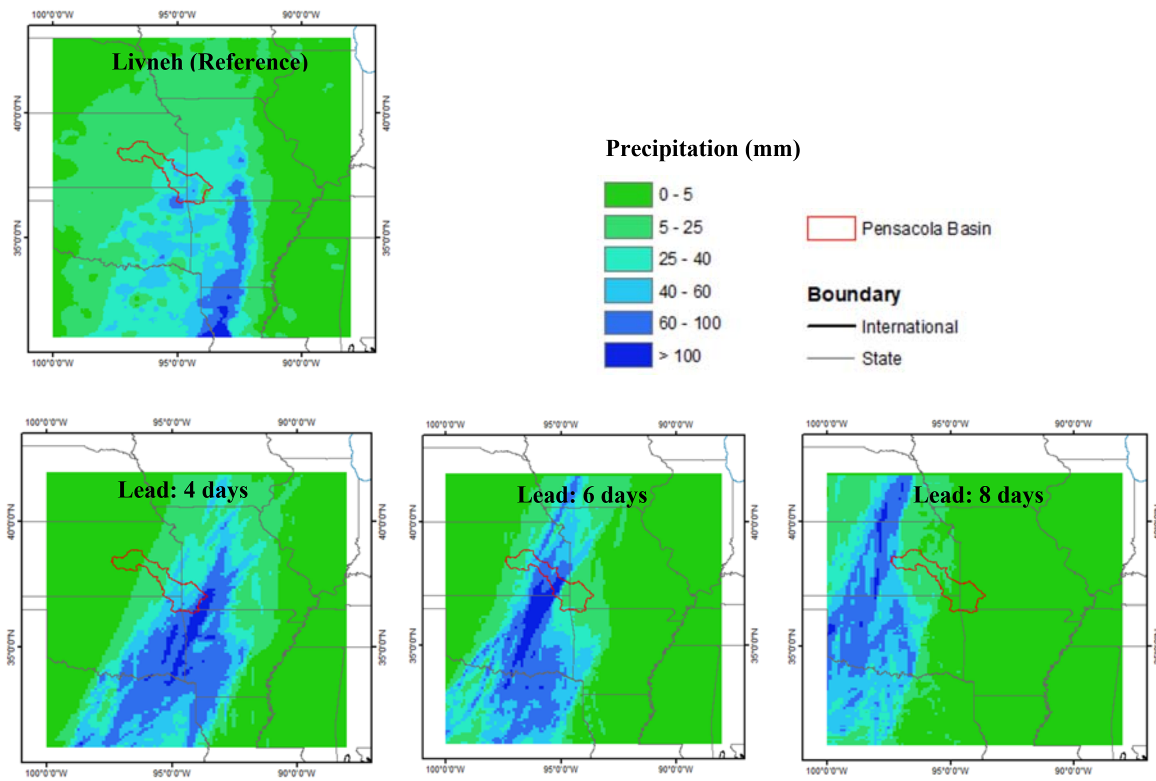

(b)

Fig. A.1. Assessment of WRF downscaled precipitation (0.1˚) with reference Livneh dataset over the events of 16 Jan 2011 and 20 Mar 2012 for (a) Detroit and (b) Pensacola dam.

Appendix B. VIC Model Setup

Detroit Dam

Calibration was performed on the period from 2009-11, and the validation over 2013-15. The first few months were ignored for calculating metrics considering the model spin-up period. Normalized RMSE is calculated as $\frac{RMSE}{\sigma_{obs}}$ (where σ_{obs} is standard deviation of the observed streamflow). The results for calibration and validation are shown in Fig. B1. As the high flow events are of interest, normalized mean absolute error ($NMAE = \frac{1}{Num\ of\ peaks}\sum\frac{|Obs-Mod|}{Mod}$) specific to peaks (with flow exceeding turbine capacity of 9000 cfs) and percentage of times peaks were under/overestimated are also shown in Fig. B1.

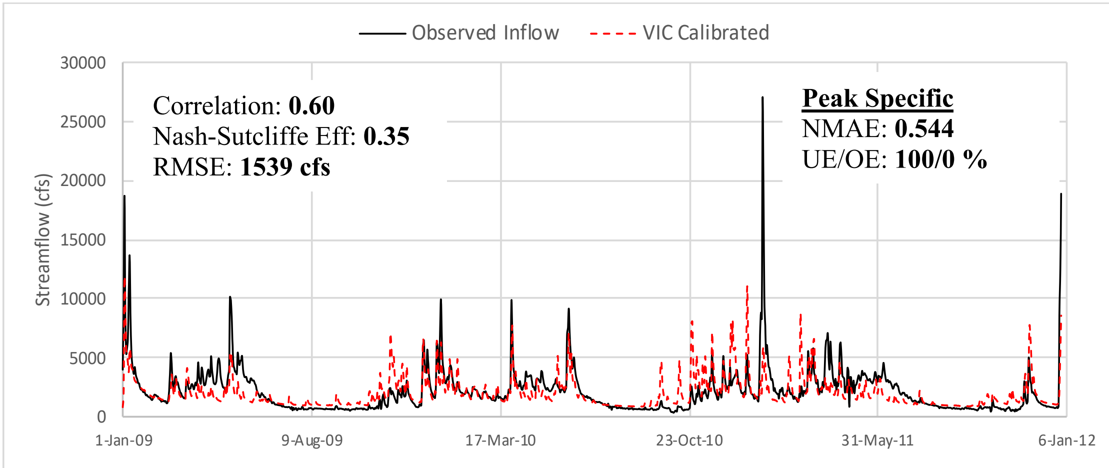

(a)

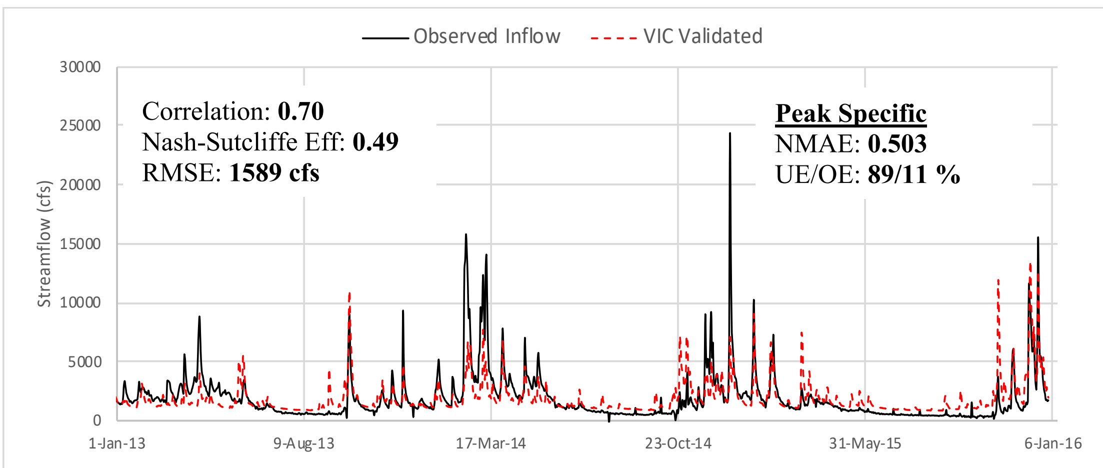

(b)

Fig. B.1. (a) VIC calibrated and (b) validated streamflow, along with metrics for Detroit Dam. NMAE is normalized mean absolute error, UE/OE is % times peak is under/overestimated.

Pensacola Dam

Daily inflow data from 2002-06 was used for calibration, while validation was performed over 2011-15. The calibration and validation results are shown below in Fig. B2. The NMAE and percent times peak is overestimated (false positive) or underestimated (missed bias) over the considered period is obtained for events with flow exceeding 20,000cfs.

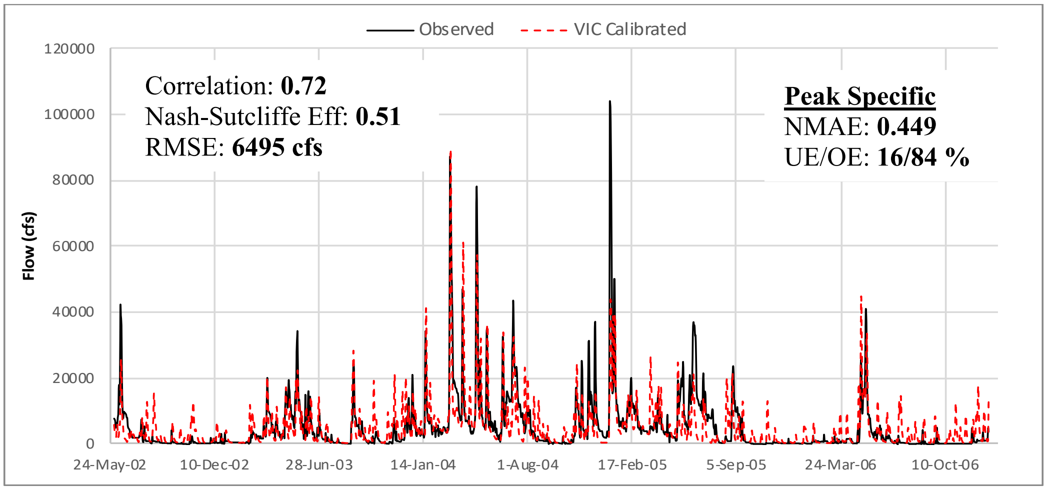

(a)

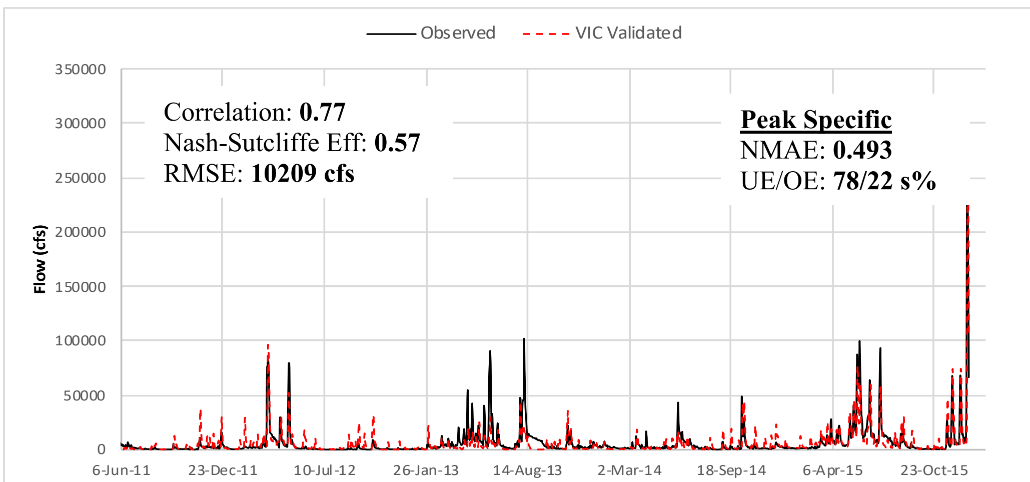

(b)

Fig. B.2. (a) VIC calibrated and (b) validated streamflow, with metrics for Pensacola Dam. NMAE is normalized mean absolute error, UE/OE is % times peak is under/overestimated.

The performance of VIC model for Pensacola dam was better compared to that of Detroit dam. Running this macroscale model at 0.1˚ resolution for smaller basin of Detroit dam results in very few grid cells that cannot capture the sub-grid heterogeneity for modeling the hydrologic variables.

Appendix C. Constraints for Optimization

1. Release from the turbines is constrained by the turbine capacity, P_{turb}.

$$R_{p,t} \leq P_{turb} \quad ,\forall t \qquad \text{Eq. (C.1)}$$

2. The system follows storage-volume continuity (water-balance equation) which requires that in each period t,

$$S_{t+1} = S_t + [I_t - L_t - (R_{p,t} + R_{np,t})] \cdot \Delta t, \ \forall t \qquad \text{Eq. (C.2)}$$

However, as the optimization is performed at daily time steps ($\Delta t = 1$), the losses due to evaporation and seepage, L_t, were ignored.

3. Reservoir storage (S) was limited to ensure dam safety and avoid infeasible scenarios such as the reservoir running empty,

$$S_{min} \leq S_t \leq S_{max}, \ \forall t = 1,2, \dots ,16 \qquad \text{Eq. (C.3)}$$

4. Daily hydropower production (HP) was limited by the powerplant's overload capacity (HP_{max}),

$$HP_t < HP_{max}, \ \forall t = 1,2, \dots ,16 \qquad \text{Eq. (C.4)}$$

5. To prevent the downstream flooding hazards, the total release was constrained to a maximum limit, R_{max},

$$R_{p,t} + R_{np,t} \leq R_{max}, \forall t \qquad \text{Eq. (C.5)}$$

6. To avoid excessive and infeasible rates of non-power release via the spillway, the non-power release rate was limited to the spillway capacity,

$$R_{np,t} \leq Spill_{max}, \ \forall t \qquad \text{Eq. (C.6)}$$

7. Lastly, the releases made from reservoir should comply with the environmental flow limit, Q_{env},

$$R_{np,t} + R_{p,t} \geq Q_{env}, \forall t \qquad \text{Eq. (C.7)}$$

Acknowledgement: The authors acknowledge the guidance and contribution of Dr. Chris Frans of US Army Corps of Engineers (USACE) Seattle District.

References

[1] M.Z. Jacobson, M.A. Delucchi, Z.A.F. Bauer, S.C. Goodman, W.E. Chapman, et al., 100% Clean and Renewable Wind, Water, and Sunlight All-Sector Energy Roadmaps for 139 Countries of the World, Joule. 1 (2017) 108–121. doi:10.1016/j.joule.2017.07.005.

[2] Hydropower Vision: A New Chapter for America's 1st Renewable Electricity Source | Department of Energy, (2016). https://www.energy.gov/eere/water/articles/hydropower-vision-new-chapter-america-s-1st-renewable-electricity-source (accessed November 21, 2016).

[3] F. Vieira, H.M. Ramos, Optimization of operational planning for wind/hydro hybrid water supply systems, Renew. Energy. 34 (2009) 928–936. doi:10.1016/j.renene.2008.05.031.

[4] M.Z. Jacobson, Review of solutions to global warming, air pollution, and energy security, Energy Environ. Sci. 2 (2009) 148–173. doi:10.1039/b809990c.

[5] M.Z. Jacobson, M.A. Delucchi, A.R. Ingraffea, R.W. Howarth, G. Bazouin, et al., A roadmap for repowering California for all purposes with wind, water, and sunlight, Energy. 73 (2014) 875–889. doi:10.1016/j.energy.2014.06.099.

[6] M.Z. Jacobson, M.A. Delucchi, M.A. Cameron, B. V. Mathiesen, Matching demand with supply at low cost in 139 countries among 20 world regions with 100% intermittent wind, water, and sunlight (WWS) for all purposes, Renew. Energy. 123 (2018) 236–248. doi:10.1016/j.renene.2018.02.009.

[7] M.Z. Jacobson, M.A. Delucchi, Providing all global energy with wind, water, and solar power, Part I: Technologies, energy resources, quantities and areas of infrastructure, and materials, Energy Policy. 39 (2011) 1154–1169. doi:10.1016/j.enpol.2010.11.040.

[8] D. Heide, L. von Bremen, M. Greiner, C. Hoffmann, M. Speckmann, S. Bofinger, Seasonal optimal mix of wind and solar power in a future, highly renewable Europe, Renew. Energy. 35 (2010) 2483–2489. doi:10.1016/j.renene.2010.03.012.

[9] M.A. Delucchi, M.Z. Jacobson, Providing all global energy with wind, water, and solar power, Part II: Reliability, system and transmission costs, and policies, Energy Policy. 39 (2011) 1170–1190. doi:10.1016/j.enpol.2010.11.045.

[10] S. Becker, B.A. Frew, G.B. Andresen, T. Zeyer, S. Schramm, M. Greiner, M.Z. Jacobson, Features of a fully renewable US electricity system: Optimized mixes of wind and solar PV and transmission grid extensions, Energy. 72 (2014) 443–458. doi:10.1016/j.energy.2014.05.067.

[11] M.Z. Jacobson, M.A. Delucchi, Providing all global energy with wind, water, and solar power, Part I: Technologies, energy resources, quantities and areas of infrastructure, and materials, (2011). doi:10.1016/j.enpol.2010.11.040.

[12] U.S. Energy Information Administration, Electric Power Monthly: with data for June 2018, Washington DC, 2018. doi:10.2172/123200.

[13] A.F. Hamlet, D. Huppert, D.P. Lettenmaier, Economic Value of Long-Lead Streamflow Forecasts for Columbia River Hydropower, J. Water Resour. Plan. Manag. 128 (2002) 91–101. doi:10.1061/(ASCE)0733-9496(2002)128:2(91).

[14] J. Spector, The Environmentalist Case Against 100% Renewable Energy Plans - CityLab, (2015). https://www.citylab.com/environment/2015/07/the-environmentalist-case-against-100-renewable-energy-plans/398906/ (accessed March 19, 2017).

[15] B. Sørensen, A combined wind and hydro power system, Energy Policy, 9 (1981), 51-55.

[16] D. Egré, J.C. Milewski, The diversity of hydropower projects, Energy Policy, 30 (2002), 1225-1230.

[17] I. Kougias, S. Szabó, F. Monforti-Ferrario, T. Huld, K. Bódis, A methodology for optimization of the complementarity between small-hydropower plants and solar PV systems, Renew. Energy. 87 (2016) 1023–1030. doi:10.1016/j.renene.2015.09.073.

[18] T. Grumet, How Germany's Combined Wind And Hydropower Plant Will Work - GE, (2016). https://www.ge.com/reports/unique-combo-wind-hydro-power-revolutionize-renewable-energy/ (accessed December 3, 2017).

[19] Hydropower Vision: A New Chapter for America's 1st Renewable Electricity Source | Department of Energy, (2016). https://www.energy.gov/eere/water/articles/hydropower-vision-new-chapter-america-s-1st-renewable-electricity-source (accessed October 12, 2017).

[20] Y. Miao, X. Chen, F. Hossain, Maximizing hydropower generation with observations and numerical modeling of the atmosphere, J. Hydrol. Eng. 21 (2016) 2516002. doi:10.1061/(ASCE)HE.1943-5584.0001405.

[21] J.W. Labadie, Optimal Operation of Multireservoir Systems: State-of-the-Art Review, J. Water Resour. Plan. Manag. 130 (2004) 93–111. doi:10.1061/(ASCE)0733-9496(2004)130:2(93).

[22] P. Block, Tailoring seasonal climate forecasts for hydropower operations, Hydrol. Earth Syst. Sci. 15 (2011) 1355–1368. doi:10.5194/hess-15-1355-2011.

[23] S.-Y. Lee, A.F. Hamlet, C.J. Fitzgerald, S.J. Burges, Optimized Flood Control in the Columbia River Basin for a Global Warming Scenario, J. Water Resour. Plan. Manag. 135 (2009) 440–450. doi:10.1061/(ASCE)0733-9496(2009)135:6(440).

[24] A. Ficchì, L. Raso, D. Dorchies, F. Pianosi, P. Malaterre, P. Van Overloop, Optimal Operation of the Multireservoir System in the Seine River Basin Using Deterministic and Ensemble Forecasts, J. Water Resour. Plan. Manag. 142 (2016) 5015005. doi:10.1061/(ASCE)WR.1943-5452.0000571.

[25] P. Bauer, A. Thorpe, G. Brunet, The quiet revolution of numerical weather prediction, Nature. 525 (2015) 47–55. doi:10.1038/nature14956.

[26] L. Goddard, Y. Aitchellouche, W. Baethgen, M. Dettinger, R. Graham, P. Hayman, M. Kadi, R. Martínez, H. Meinke, Providing Seasonal-to-Interannual Climate Information for Risk Management and Decision-making, Procedia Environ. Sci. 1 (2010) 81–101. doi:10.1016/j.proenv.2010.09.007.

[27] D. Anghileri, N. Voisin, A. Castelletti, F. Pianosi, B. Nijssen, D.P. Lettenmaier, Value of long-term streamflow forecasts to reservoir operations for water supply in snow-dominated river catchments, Water Resour. Res. 52 (2016) 4209–4225. doi:10.1002/2015WR017864.

[28] K.P. Georgakakos, N.E. Graham, A.P. Georgakakos, H. Yao, Demonstrating Integrated Forecast and Reservoir Management (INFORM) for northern California in an operational environment, IAHS-AISH Publ. (2007) 439–444.

[29] FIRO_Overview – Center for Western Weather and Water Extremes, (2016). http://cw3e-web.ucsd.edu/firo/ (accessed July 31, 2017).

[30] J. Murphy, Predictions of climate change over Europe using statistical and dynamical downscaling techniques, Int. J. Climatol. 20 (2000) 489–501. doi:10.1002/(SICI)1097-0088(200004)20:5<489::AID-JOC484>3.0.CO;2-6.

[31] S. Sikder, F. Hossain, Assessment of the weather research and forecasting model generalized parameterization schemes for advancement of precipitation forecasting

in monsoon-driven river basins, J. Adv. Model. Earth Syst. 8 (2016) 1210–1228. doi:10.1002/2016MS000678.

[32] C. Teutschbein, F. Wetterhall, J. Seibert, Evaluation of different downscaling techniques for hydrological climate-change impact studies at the catchment scale, Clim. Dyn. 37 (2011) 2087–2105. doi:10.1007/s00382-010-0979-8.

[33] W.W.-G. Yeh, Reservoir Management and Operations Models: A State-of-the-Art Review, Water Resour. Res. 21 (1985) 1797–1818. doi:10.1029/WR021i012p01797.

[34] D. Rani, M.M. Moreira, Simulation–Optimization Modeling: A Survey and Potential Application in Reservoir Systems Operation, Water Resour. Manag. 24 (2010) 1107–1138. doi:10.1007/s11269-009-9488-0.

[35] A. Ahmad, A. El-Shafie, S.F.M. Razali, Z.S. Mohamad, Reservoir Optimization in Water Resources: A Review, Water Resour. Manag. 28 (2014) 3391–3405. doi:10.1007/s11269-014-0700-5.

[36] M. Yasar, Optimization of Reservoir Operation Using Cuckoo Search Algorithm: Example of Adiguzel Dam, Denizli, Turkey, Math. Probl. Eng. 2016 (2016) 1–7. doi:10.1155/2016/1316038.

[37] M.T.L. Barros, F.T.-C. Tsai, S. Yang, J.E.G. Lopes, W.W.-G. Yeh, Optimization of Large-Scale Hydropower System Operations, J. Water Resour. Plan. Manag. 129 (2003) 11. doi:10.1061/(ASCE)0733-9496(2003)129:3(178).

[38] V. Jothiprakash, R. Arunkumar, Multi-reservoir optimization for hydropower production using NLP technique, KSCE J. Civ. Eng. 18 (2014) 344–354. doi:10.1007/s12205-014-0352-2.

[39] N.S. Hsu, C.C. Wei, A multipurpose reservoir real-time operation model for flood control during typhoon invasion, J. Hydrol. 336 (2007) 282–293. doi:10.1016/j.jhydrol.2007.01.001.

[40] J.S. Windsor, Optimization model for the operation of flood control systems, Water Resour. Res. 9 (1973) 1219–1226. doi:10.1029/WR009i005p01219.

[41] Y. Ji, X. Lei, S. Cai, X. Wang, Hedging rules for water supply reservoir based on the model of simulation and optimization, Water (Switzerland). 8 (2016). doi:10.3390/W8060249.

[42] T.R. Neelakantan, N. V Pundarikanthan, Hedging Rule Optimisation for Water Supply Reservoirs System, Water Resour. Manag. 13 (1999) 409–426. doi:10.1023/A:1008157316584.

[43] P.E. Georgiou, D.M. Papamichail, Optimization model of an irrigation reservoir for water allocation and crop planning under various weather conditions, Irrig. Sci. 26 (2008) 487–504. doi:10.1007/s00271-008-0110-7.

[44] S.K. Sadati, S. Speelman, M. Sabouhi, M. Gitizadeh, B. Ghahraman, GA-Optimal irrigation water allocation using a genetic algorithm under various weather conditions, Water (Switzerland). 6 (2014) 3068–3084. doi:10.3390/w6103068.

[45] W.W.-G. Yeh, L. Becker, Multiobjective analysis of multireservoir operations, Water Resour. Res. 18 (1982) 1326–1336. doi:10.1029/WR018i005p01326.

[46] W. Ding, C. Zhang, Y. Peng, R. Zeng, H. Zhou, X. Cai, An analytical framework for flood water conservation considering forecast uncertainty and acceptable risk, Water Resour. Res. 51 (2015) 4702–4726. doi:10.1002/2015WR017127.

[47] M.J. Reddy, D.N. Kumar, Optimal Reservoir Operation Using Multi-Objective Evolutionary Algorithm, Water Resour. Manag. 20 (2006) 861–878. doi:10.1007/s11269-005-9011-1.

[48] M.J. Reddy, D. Nagesh Kumar, Multi-objective particle swarm optimization for generating optimal trade-offs in reservoir operation, Hydrol. Process. 21 (2007) 2897–2909. doi:10.1002/hyp.6507.

[49] S.T. Khu, H. Madsen, Multiobjective calibration with Pareto preference ordering: An application to rainfall-runoff model calibration, Water Resour. Res. 41 (2005). doi:10.1029/2004WR003041.

[50] L. Le Ngo, H. Madsen, D. Rosbjerg, Simulation and optimisation modelling approach for operation of the Hoa Binh reservoir, Vietnam, J. Hydrol. 336 (2007) 269–281. doi:10.1016/j.jhydrol.2007.01.003.

[51] M. Ahmadi, O. Bozorg Haddad, M.A. Mariño, Extraction of Flexible Multi-Objective Real-Time Reservoir Operation Rules, Water Resour. Manag. 28 (2014) 131–147. doi:10.1007/s11269-013-0476-z.

[52] T.E. Croley, K.N. Raja Rao, Multiobjective risks in reservoir operation, Water Resour. Res. 15 (1979) 807–814. doi:10.1029/WR015i004p00807.

[53] Query Timeseries from USACE Northwestern Division, Dataquery 2.0, (2017). http://www.nwd-wc.usace.army.mil/dd/common/dataquery/www/ (accessed October 17, 2017).

[54] Monthly Charts for Grand Lake O' The Cherokees, Pensacola Dm, (2018). http://www.swt-wc.usace.army.mil/PENScharts.html (accessed August 21, 2017).

[55] X. Chen, F. Hossain, Revisiting extreme storms of the past 100 years for future safety of large water management infrastructures, Earth's Futur. 4 (2016) 306–322. doi:10.1002/2016EF000368.

[56] W.C. Skamarock, J.B. Klemp, J. Dudhia, D.O. Gill, D.M. Barker, M.G. Duda, X.-Y. Huang, W. Wang, J.G. Powers, A Description of the Advanced Research WRF Version 3, (2008). doi:10.5065/D68S4MVH.

[57] D.J. Stensrud, Parameterization schemes: keys to understanding numerical weather prediction models, Cambridge University Press, 2007.

[58] Pacific Northwest Mesoscale Model Numerical Forecast Information, (2017). https://www.atmos.washington.edu/wrfrt/info.html (accessed November 23, 2017).

[59] X. Liang, D.P. Lettenmaier, E.F. Wood, S.J. Burges, A simple hydrologically based model of land surface water and energy fluxes for general circulation models, J. Geophys. Res. 99 (1994) 14415. doi:10.1029/94JD00483.

[60] X. Liang, E.F. Wood, D.P. Lettenmaier, Surface soil moisture parameterization of the VIC-2L model: Evaluation and modification, Glob. Planet. Change. 13 (1996) 195–206. doi:10.1016/0921-8181(95)00046-1.

[61] Global Surface Summary of the Day - GSOD - NOAA Data Catalog, (2017). https://data.noaa.gov/dataset/global-surface-summary-of-the-day-gsod (accessed August 30, 2017).

[62] D. Lohmann, R. Nolte-Holube, E. Raschke, A large-scale horizontal routing model to be coupled to land surface parametrization schemes, Tellus, Ser. A Dyn. Meteorol. Oceanogr. 48 (1996) 708–721. doi:10.3402/tellusa.v48i5.12200.

[63] D. Lohmann, E. Raschke, B. Nijssen, D.P. Lettenmaier, Regional scale hydrology: I. Formulation of the VIC-2L model coupled to a routing model, Hydrol. Sci. J. 43 (1998) 131–141. doi:10.1080/02626669809492107.

[64] H. Madsen, B. Richaud, C.B. Pedersen, C. Borden, A Real-Time Inflow Forecasting and Reservoir Optimization System for Optimizing Hydropower Production, Waterpower XVI. (2009) 1–12.

[65] K. Deb, S. Agrawal, A. Pratap, T. Meyarivan, A fast elitist non-dominated sorting genetic algorithm for multi-objective optimization: NSGA-II. International Conference on Parallel Problem Solving from Nature, Springer, Berlin, Heidelberg (2000), 849-858.

[66] F.F. Li, J. Qiu, Multi-objective reservoir optimization balancing energy generation and firm power, Energies 8 (2015), 6962–6976. doi:10.3390/en8076962.

[67] Oklahoma City, OK Electricity Rates | Electricity Local, (2018). https://www.electricitylocal.com/states/oklahoma/oklahoma-city/ (accessed August 21, 2018).

[68] Oregon Electricity Rates | Electricity Local, (2018). https://www.electricitylocal.com/states/oregon/ (accessed May 11, 2018).

[69] NHAAP | Existing Hydropower Assets, (2017). https://nhaap.ornl.gov/existing_hydropower_assets (accessed December 8, 2017).

[70] B. Livneh, E.A. Rosenberg, C. Lin, B. Nijssen, V. Mishra, K.M. Andreadis, E.P. Maurer, D.P. Lettenmaier, A Long-Term Hydrologically Based Dataset of Land Surface Fluxes and States for the Conterminous United States: Update and Extensions, J. Clim. 26 (2013) 9384–9392. doi:10.1175/jcli-d-12-00508.1.

[71] W.H. Farmer, R.M. Vogel, On the deterministic and stochastic use of hydrologic models, Water Resour. Res. 52 (2016) 5619-5633. doi:10.1002/2016WR019129.

[72] F. Hossain, A.M. Degu, W. Yigzaw, S. Burian, D. Niyogi, J.M. Shepherd, R. Pielke, Climate Feedback–Based Provisions for Dam Design, Operations, and Water Management in the 21st Century, J. Hydrol. Eng. 17 (2012) 837–850. doi:10.1061/(ASCE)HE.1943-5584.0000541.

[73] B. Lehner, B., C.R. Liermann, C. Revenga, C. Voro Smarty, B. Fekete, P. Crouzet et al., Global reservoir and dam (GRanD) database, Version 1.1 (2011) Bonn, Germany: Global Water System Project.

[74] G.M. Sechi, A. Sulis, Water System Management through a Mixed Optimization-Simulation Approach, J. Water Resour. Plan. Manag. 135 (2009) 160–170. doi:10.1061/(ASCE)0733-9496(2009)135:3(160).

[75] E.T. Alemu, R.N. Palmer, A. Polebitski, B. Meaker, Decision Support System for Optimizing Reservoir Operations Using Ensemble Streamflow Predictions, J. Water Resour. Plan. Manag. 137 (2011) 72–82. doi:10.1061/(ASCE)WR.1943-5452.0000088.

[76] Global Forecast System (GFS) | National Centers for Environmental Information (NCEI) formerly known as National Climatic Data Center (NCDC), (2018). https://www.ncdc.noaa.gov/data-access/model-data/model-datasets/global-forcast-system-gfs (accessed December 30, 2017).